The specific heat of $ErNi_5$ and $LaNi_5$

1992 J. Phys.: Condens. Matter 4 8853

(http://iopscience.iop.org/0953-8984/4/45/018)

J. Phys.: Condens. Matter 4 (1992) 8853–8862. Printed in the UK

The specific heat of $ErNi_5$ and $LaNi_5$

R J Radwański†§, N H Kim-Ngan†||, F E Kayzel†, J J M Franse†, D Gignoux‡, D Schmitt‡ and F Y Zhang‡

† Van der Waals–Zeeman Laboratorium, Universiteit van Amsterdam, Valckenierstraat 65, 1018 XE Amsterdam, Netherlands

‡ Laboratoire Louis Néel, CNRS, 166X 38042 Grenoble Cédex, France

Received 26 June 1992

Abstract. The specific heat of $ErNi_5$ and $LaNi_5$ has been measured on single-crystalline specimens in the temperature interval from 1.5 K to 250 K. By comparison, the contribution of the Er subsystem to the specific heat has been determined. This contribution is well accounted for within a single-ion Hamiltonian that includes the CEF and exchange interactions of the Er^{3+} ions. The CEF interactions of the Er^{3+} ion have been compared with those found in other RNi_5 compounds and the remarkable constancy of CEF interactions through the 4f series is discussed.

1. Introduction

$ErNi_5$ crystallizes in a hexagonal crystallographic structure and orders ferrimagnetically below 9 K [1]. Magnetization studies performed in fields up to 35 T along the c and a axes of $ErNi_5$ [2] have resulted in the Γ_9 doublet with a dominant $|\pm 15/2\rangle$ component as the ground state of the Er^{3+} ion in agreement with inelastic neutron scattering (INS) experiments performed by Goremychkin *et al* [3]. Specific heat studies of $ErNi_5$ have been undertaken in order to resolve the controversy concerning the magnetic/CEF contribution to the specific heat of the Er subsystem in this compound. The single-ion contribution due to the presence of the Er^{3+} ion in $ErNi_5$ calculated in [2] has been found to be significantly larger than derived experimentally in [4]. This discrepancy has been attributed to uncertainties in the experimental evaluation of the Er-subsystem specific heat probably associated with the approximations used in the determination of the phonon contribution. In this paper, we present our results of specific heat measurements on $ErNi_5$ and $LaNi_5$. This latter compound serves as the reference system, having the same crystallographic structure and containing a non-magnetic rare-earth element.

2. Experimental details

The specific heat of $ErNi_5$ has been measured on a single-crystalline specimen with a mass of 190 mg in the temperature range from 1.5 K to 250 K by an adiabatic

§ Present address: Centre for Solid State Physics, Filipa 5/5, 31-150 Krakow, Poland.

|| On leave from: Cryogenic Laboratory of the University of Hanoi, Vietnam.

0953-8984/92/458853+10$07.50

method. This single-crystalline specimen is part of a single-crystalline batch that has been grown by the arc-melting technique in a purified argon atmosphere at the Material Centre ALMOS of the University of Amsterdam. The quality of the sample is found to be high—the presence of erbium oxide is not detectable. Er_2O_3 is manifest in the specific heat by a peak at the magnetic ordering temperature of 3.2 K. In the present measurement no anomaly at this temperature is observed. For $LaNi_5$, the specimen consists of three pieces of single-crystalline material with a total mass of 253 mg.

3. Results and discussion

The specific heat of $ErNi_5$ is shown in figure 1, together with that of $LaNi_5$. The specific heat of $ErNi_5$ is much larger than that of $LaNi_5$. The λ-type of peak of the $ErNi_5$ with its maximum at 8.9 K is associated with the occurrence of long-range magnetic order. The value of 9.2 K for T_c is taken from the mid-point temperature of the λ-peak. The specific heat is analysed by taking into account the nuclear (c_N), electronic (c_{el}), lattice (phonon) (c_{ph}) and magnetic (c_m) contributions to the specific heat:

$$c = c_N + c_{el} + c_{ph} + c_m. \tag{1}$$

The nuclear contribution, related to hyperfine interactions of the 4f shell with the nuclear moment of the 4f ion, is not observed. This is not surprising as even in the case of a fully polarized 4f shell of the Er ion, the nuclear specific heat contributes significantly only below 1 K.

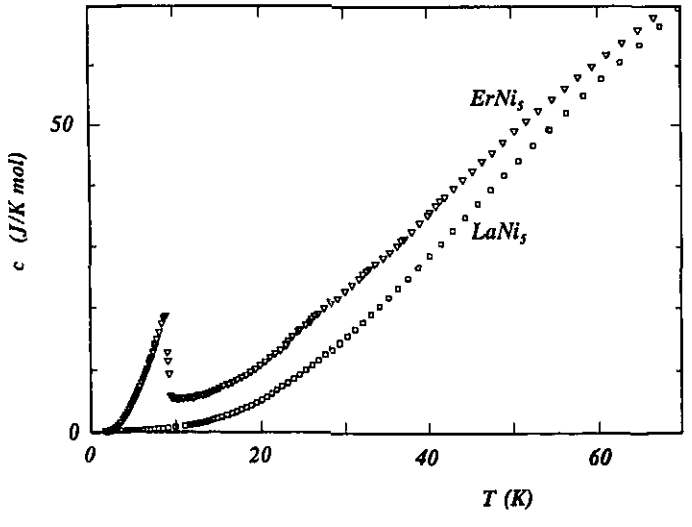

Figure 1. Specific heat of single-crystalline $ErNi_5$ and $LaNi_5$.

Information about the electronic and lattice contributions is provided by the specific heat of $LaNi_5$, a compound that is Pauli paramagnetic. The specific heat

of this compound is shown in figure 2. It shows a smooth behaviour, resembling the Debye function. At a temperature of 220 K it reaches the value of $18R$, R being the gas constant. The behaviour at low temperatures is presented in more detail in figure 3 in a plot of c/T versus T^2. This plot clearly does not follow a linear variation, implying that the phonon contribution does not follow the Debye function temperature dependence in detail. Apparently, the dynamics of the lattice cannot be described over the full temperature range by one single parameter, the Debye temperature. We have correlated this fact with a complex energy structure of the phonon spectrum that has been revealed by point-contact spectroscopy measurements performed by Akimenko *et al* [5]. In fact, the specific heat of $LaNi_5$ can be represented by a straight line in temperature up to 10 K only. The low-temperature variation shown in figure 3 leads to a Sommerfeld coefficient γ of 36 mJ K^{-2} mol^{-1} and θ_D of 322 K. The specific heat for $LaNi_5$ has been measured before by Nait-Saada [6] and Sahling *et al* [7] who reported values of 33 and 39 mJ K^{-2} mol^{-1} for γ and values of 322 and 393 K for the Debye temperature θ_D, respectively. Values of 36 mJ K^{-2} mol^{-1} and 296 K for γ and θ_D have been found by Szewczyk *et al* [8] from specific heat measurements of $GdNi_5$. From a detailed analysis over different temperature regions of the specific heat of $LaNi_5$, we deduced a variation of the Debye temperature with temperature. This variation is shown in the inset of figure 3. The value reported in [8], which has been derived within the temperature region between 35 and 45 K falls well in this variation. Apparently, there is a significant phonon softening at 22 K. We have correlated this variation of θ_D with the non-standard phonon spectrum revealed by point-contact spectroscopy measurements.

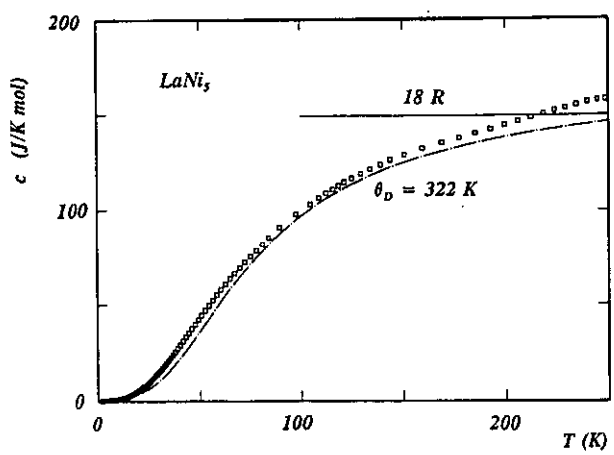

Figure 2. Experimental specific heat of single-crystalline $LaNi_5$, together with an approximation made with a Debye temperature θ_D of 322 K and γ of 36 mJ K^{-2} mol^{-1} (chain curve). The horizontal line represents a value of $18R$.

Leaving the problem of the detailed analysis of the phonon contribution in $LaNi_5$ out of the present discussion, the contribution of the Er subsystem in $ErNi_5$ has been derived as the difference of the measured (molar) specific heats of $ErNi_5$ and $LaNi_5$.

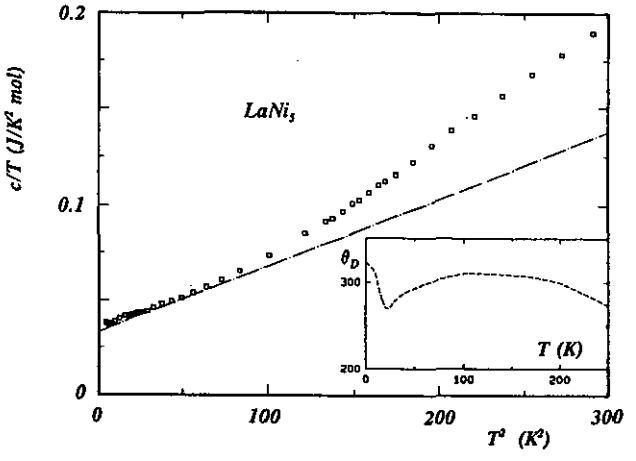

Figure 3. Experimental specific heat of $LaNi_5$ at low temperatures shown in a plot of c/T versus T^2. The chain curve represents the heat calculated with the Debye function with θ_D of 322 K and with γ of 36 mJ K^{-2} mol^{-1}. In the inset the derived temperature variation of θ_D is shown.

This contribution is shown in figure 4. Already, at a first glance, this contribution (i) is much larger than that derived in [4] (see also figure 3 of [2]) and (ii) resembles well the calculated specific heat that has been presented in [2]. This confirms the suggestion that the lattice contribution was not subtracted correctly in [4]. We have calculated the entropy that is involved in this extra specific heat. Its temperature variation is shown in figure 5. At 150 K it reaches a value of 21.5 ± 1 J K^{-1} mol^{-1} with zero entropy at 1.3 K. This value is close to that expected for the $(2J + 1)$-fold degeneracy of the ground multiplet, i.e. $R \ln 16 = 23.04$ J K^{-1} mol^{-1}. It indicates that (i) this extra specific heat observed in $ErNi_5$ is associated with the electronic excitations of the Er^{3+} ions, and (ii) that the magnitude of the CEF interactions in $ErNi_5$ is of the order of 150 K.

The rare-earth specific heat is calculated by making use of the general formula:

$$c_m = -T\delta^2 F/\delta T^2. \tag{2}$$

F is the free energy of the rare-earth subsystem over the available energy states resulting from the consideration of the Hamiltonian of the Er^{3+} ion in the form:

$$\mathcal{H}_R = \sum\sum B_n^m O_n^m + ng^2\mu_B^2\left(-J\langle J\rangle + \tfrac{1}{2}\langle J\rangle^2\right). \tag{3}$$

The first term is the CEF Hamiltonian written for the lowest multiplet given by Hund's rules: $^4I_{15/2}$ with $J = 15/2$, $S = 3/2$, $L = 6$ and the Landé factor $g = 6/5$. The second term represents the exchange interactions between the Er ions written in the mean-field approximation. The calculated contribution of the Er^{3+} ions to the specific heat of $ErNi_5$ is shown in figure 4. The overall behaviour is in very good agreement with the experimentally derived magnetic contribution to the specific heat. It perfectly reproduces (i) the λ-type of peak at 8.9 K associated with the occurrence

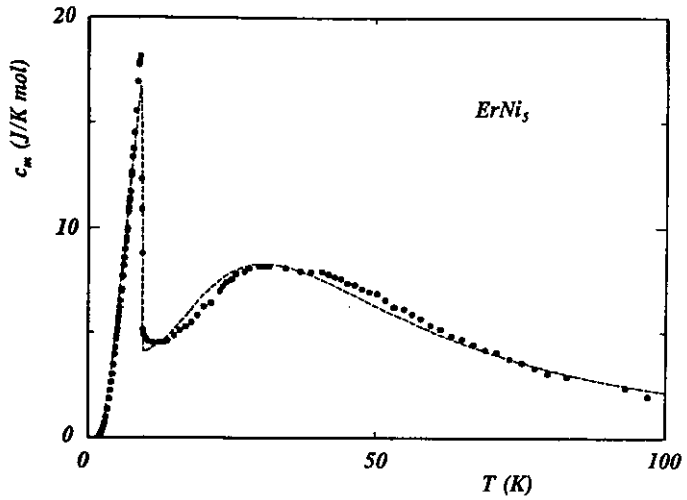

Figure 4. Temperature variation of the contribution of the Er subsystem to the specific heat of $ErNi_5$ derived as the difference of the molar specific heats of $ErNi_5$ and $LaNi_5$. The broken curve shows the Er-subsystem contribution calculated with the CEF parameters shown in table 1 under [2]. The value for the effective molecular field coefficient n_{RR} between the Er moments of 0.17 T f.u./μ_B determines the position of the λ-type of peak with $T_c = 9.2$ K.

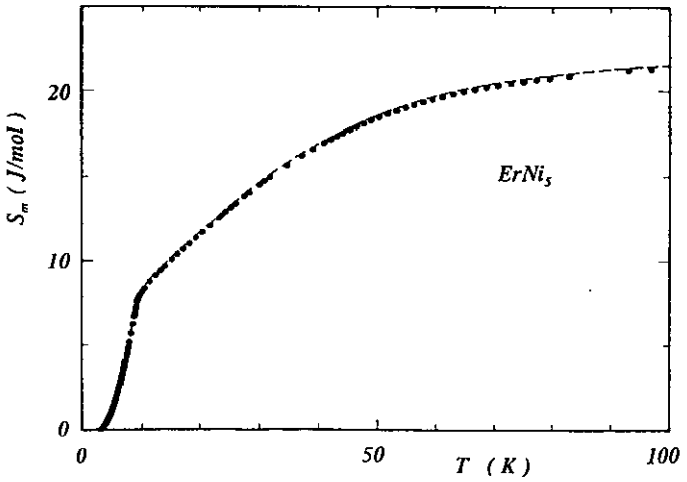

Figure 5. Temperature variation of the experimental entropy of the Er subsystem. The entropy associated with the excitations of the 4f electrons over the Hund's ground-state multiplet amounts to 23.04 J K^{-1} mol^{-1}.

of long-range magnetic order and (ii) the broad Schottky-type of maximum in the vicinity of 30 K. The calculated value of the maximum amounts to 8.3 J K^{-1} mol^{-1}, whereas the experimental results point to a broader maximum with a maximal value of 7.3 J K^{-1} mol^{-1}. In principle, the better fit could be obtained by relatively

small variations of the energy separations. This has not been done, however, owing to the fact that the specific heat is insensitive to the eigenfunctions of the states. Detailed magnetic measurements and high-resolution inelastic neutron scattering on well characterized single-crystalline specimens are planned.

The set of CEF parameters, relevant to the hexagonal symmetry that has been used in these calculations, has been taken from [2]. This set of parameters describes well

(i) the energy separations to the three lowest levels (i.e. the INS results of [3]);
(ii) the spontaneous moment of the Er ion close to 9 μ_B;
(iii) the ground state of the Er^{3+} ion;
(iv) the anisotropy of the susceptibility;
(v) the temperature dependence of the susceptibility with a 'bump' at 20 K for the direction perpendicular to the hexagonal axis (figure 4 of [2]);
(vi) the magnetization in high fields; and
(vii) the temperature dependence of the specific heat of the Er subsystem.

This set of CEF parameters is shown in table 1, together with those obtained in [1] and [3]. In principle, one can see that for all the sets there is a general agreement over the size of the CEF interactions and the parameters themselves are quite similar. The set from [1] leads, however, to the ground state Γ_7, that must be excluded on the basis of the magnetization measurements in high fields [2] as well as of INS experiments [3].

Table 1. Crystal field parameters B_n^m of the Er^{3+} ion in $ErNi_5$. The overall splitting as well as the ground state of the Er^{3+} ion, due to the crystal field interactions of hexagonal symmetry, are also shown.

B_n^m	[1]	[3]	[2]
B_2^0 (K)	−0.7	−0.64	−0.615
B_4^0 ($\times 10^{-3}$ K)	−1	−2.3	−2.5
B_6^0 ($\times 10^{-6}$ K)	+50	+23.2	+23.2
B_6^6 ($\times 10^{-6}$ K)	+300	+132	+132
Ground state	Γ_7	Γ_9	Γ_9
CEF splitting (K)	183	151	152

The anisotropic behaviour of the paramagnetic susceptibility of the Er subsystem has been calculated in [2]. The temperature dependences of the inverse susceptibility along the hard and easy axes above 100 K follow the Curie–Weiss law very well. Both curves show nearly the same value of the paramagnetic moment ($p_\parallel = 9.62\ \mu_B, p_\perp = 9.71\ \mu_B$) but the paramagnetic Curie temperatures differ by 54 K ($\theta_\parallel = +28$ K and $\theta_\perp = -26$ K). The contribution of the Er subsystem accounts for most of the susceptibility of $ErNi_5$. Even at 300 K the Er subsystem susceptibility largely exceeds that associated with the conduction electrons, which predominantly originate from the Ni subsystem. The anticipated 'bump' in the vicinity of 20 K in the susceptibility for the $c \perp$ direction seen in figure 4 of [2], that has not been observed in measurements reported in [1] and [6], has been found in recent susceptibility measurements [9].

The energy level scheme of the Er^{3+} ion, calculated with the present set of CEF parameters, is shown in figure 6, together with the associated eigenfunctions. The CEF interactions of the hexagonal symmetry split the $^4I_{15/2}$ multiplet into eight doublets as

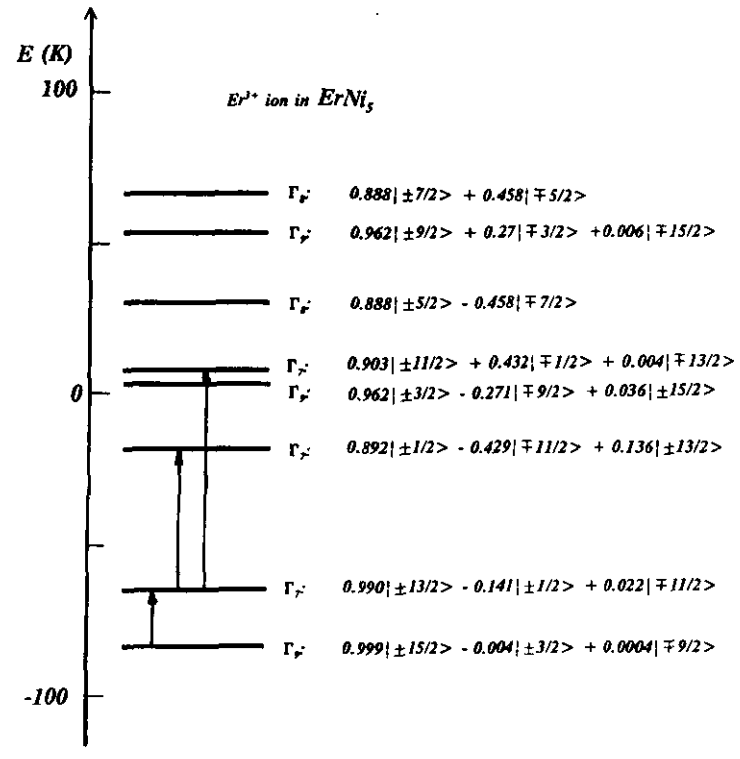

Figure 6. The energy level scheme of the Er^{3+} ion in $ErNi_5$ under the action of the CEF interactions, the CEF parameters are shown in table 1 under [2], together with the associated eigenfunctions. All the levels are doublets, as the Er^{3+} ion with $J = 15/2$ is a Kramers ion. The arrows show the transitions observed in inelastic neutron scattering experiments.

the Er^{3+} ion, with $J = 15/2$, is a Kramers ion. The eigenfunction of the ground-state doublet Γ_9 is given by:

$$\psi = +0.999|\pm 15/2\rangle - 0.04|\pm 3/2\rangle + 0.0004|\mp 9/2\rangle. \tag{4}$$

The quantization axis is taken along the hexagonal axis. The largest component is given by the maximal value of J_z. This ground state results from predominant second-order CEF interactions. The energy level scheme with eigenfunctions as shown in figure 6 provides excitations observable in INS experiments at energies of 21.0 K ($1 \rightarrow 2$), 46.0 K ($2 \rightarrow 3$) and 72.6 K ($2 \rightarrow 5$). These excitations have been observed [3].

In the ordered state all the levels are split by the exchange interactions but their splitting is small. In figure 7 the temperature dependence of the energy level scheme is presented. The exchange interactions do not cause a mixing of the levels. The effective molecular field coefficient between the Er-ion moments, n, has been found to be 0.17 T f.u./μ_B [2]. This is 15% lower than the value of 0.20 T f.u./μ_B that can be derived from the molecular field expression

$$n = 3k_B T_c / g^2 \mu_B^2 J(J+1). \tag{5}$$

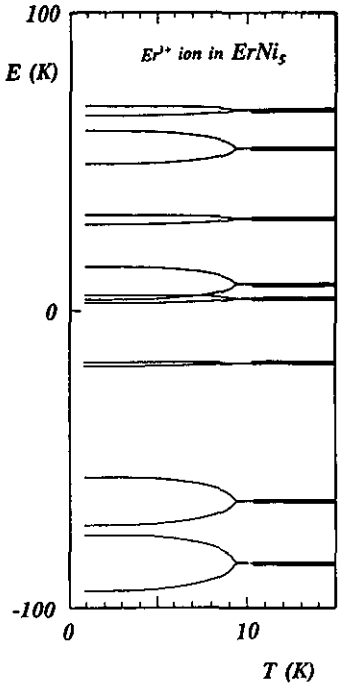

Figure 7. Effect of the exchange interactions on the energy level scheme of the Er^{3+} ion in $ErNi_5$. The splitting of the doublets in the magnetically ordered state, $T_c = 9.2$ K, does not mix the lowest levels.

Exchange interactions of this size produce a molecular field of 1.5 T experienced by the Er^{3+}-ion moment at the lowest temperatures.

It is interesting to compare the CEF interactions in $ErNi_5$ with those evaluated on the basis of numerous magnetic, neutron and specific heat studies, for other R^{3+} ions within the RNi_5 series. This comparison is made in table 2, where the values for CEF coefficients, $A_n^m = B_n^m/\theta_n\langle r_{4f}^n\rangle$, are collected. θ_n is the nth-order Stevens factor, whereas $\langle r_{4f}^n\rangle$ is the nth power of the radius of the 4f shell. Values for the multipolar charge moments of the 4f electron cloud $\theta_n\langle r_{4f}^n\rangle$ have been collected in [10]. Inspecting the results shown in table 2, one can notice, on the one hand, a substantial difference between the coefficients in different compounds but, on the other hand, remarkable systematics can be found. Except for the coefficient A_6^0 of the Tm ion, there is full agreement in the sign of the CEF coefficients across the series. The nearly constant CEF interactions in the RNi_5 series independently on the R ion involved result in (i) a systematic uniaxial/planar alternation of the easy magnetic direction (EMD) (governed by the sign of the second-order Stevens factor α_J) and (ii) a systematic a/b axis alternation of the EMD within the hexagonal plane (governed by the sign of the sixth-order Stevens factor γ_J). These systematic alternations are also found in other series like the hexagonal R_2Co_{17} and R_2Fe_{17}, and the cubic RFe_2 compounds, and have been discussed in [19].

4. Conclusions

The temperature dependence of the specific heat of $ErNi_5$ is well understood by considering two independent electronic subsystems. The conduction electron subsystem is described by a value for the Sommerfeld coefficient γ of 36 mJ K^{-2} mol^{-1}. The substantial departure of the lattice contribution to the specific heat from that

Table 2. CEF coefficients, in units of Ka_0^{-n}, of the trivalent R ions in the RNi_5 compounds. PCM denotes a point charge model result.

Compound	T_c (K)	A_2^0	A_4^0	A_6^0	A_6^6	Reference
$PrNi_5$	—	−229	−18.2	+0.78	+27.5	[11]
$PrNi_5$	—	−227	−20.8	+0.7	+27.1	[12]
$NdNi_5$	8	−468	−17.1	+0.61	+23.6	[13]
$SmNi_5$	27	−370	−181	+11.4	0.0	[14]
$GdNi_5$	32					[8]
$TbNi_5$	23	−385	−13.4	+5.8	+13.0	[15]
$TbNi_5$		−442	−9.0	+1.5	+47.7	[3]
$TbNi_5$		−462	−11.9	+0.79	+47.7	[16]
$DyNi_5$	12	−458	−24.7	+1.8	+45.0	[17]
$HoNi_5$	5	−686	−56	+0.3	+55.0	[15]
$ErNi_5$	9	−382	−17.7	+5.0	+30.0	[1]
$ErNi_5$		−349	−40.0	+2.4	+13.7	[3]
$ErNi_5$	9.2	−336	−44.3	+2.3	+13.7	[2]
$TmNi_5$	5	−545	−65.8	−7.52	+31.2	[18]
RNi_5 (PCM)		−300	−10.0	−0.06	−0.39	[15]
$SmNi_5$ (PCM)		−422	−11.0	−0.07	−0.43	[14]

given by the Debye function has been deduced from measurements on $LaNi_5$. The 4f electronic subsystem of the Er ions is well accounted for by the CEF and effective Er–Er exchange interactions. The CEF interactions of the R^{3+} ions in RNi_5 derived from a large number of magnetic, neutron and specific heat studies are found to be remarkably similar and independent of the R^{3+} ion involved.

Acknowledgments

This work has been partly supported by the European Commission within its BRITE/EURAM Research and Development Programme, BREU-0068.

References

[1] Escudier P, Gignoux D, Givord D, Lemaire R and Murani A P 1977 *Physica* B **86 & 88** 197
[2] Radwański R J, Franse J J M, Gignoux D, Kayzel F E, Marquina C and Szewczyk A 1992 *Physica* B **177** 291
[3] Goremychkin E A, Mühle E, Ivanitskii P G, Krotenko V T, Pasechnik M V, Slisenko V V, Vasilkevich A A, Lippold B, Chistyakov O D and Savitskii E M 1984 *Phys. Status Solidi* b **121** 623
[4] Sankar S G, Keller D A, Craig R S, Wallace W E and Rao V U S 1974 *J. Solid State Chem.* **9** 78
[5] Akimenko A I, Ponomarenko N M and Yanson I K 1986 *Fiz. Tverd. Tela* **28**; 1986 *Sov. Phys.–Solid State* **28** 615
[6] Nait-Saada A 1980 *Thesis* University of Grenoble
[7] Sahling A, Frach P and Hegenbarth E 1982 *Phys. Status Solidi* b **112** 243
[8] Szewczyk A, Radwański R J, Franse J J M and Nakotte H 1992 *J. Magn. Magn. Mater.* **104–7** 1319
[9] Gignoux D *et al* to be published
[10] Radwański R J and Franse J J M 1989 *Physica* B **154** 181
[11] Barthem V M T S, Gignoux D, Nait-Saada A and Schmitt D 1988 *Phys. Rev.* B **37** 1733
[12] Reiffers M, Naidyuk Yu G, Jansen A G M, Wyder P and Yanson I K 1989 *Phys. Rev. Lett.* **62** 1560
[13] Barthem V M T S, Gignoux D, Nait-Saada A, Schmitt D and Takeuchi A Y 1989 *J. Magn. Magn. Mater.* **80** 142
[14] Ballou R, Barthem V M T S and Gignoux D 1988 *Physica* B **149** 340

[15] Gignoux D, Nait-Saada A, Perrier de la Bâthie R and Sayetat F 1979 *J. Phys. F: Met. Phys.* **9** 763
[16] Gignoux D and Rhyne J J 1986 *J. Magn. Magn. Mater.* **54–57** 1179
[17] Aubert G, Gignoux D, Hennion B, Michelutti B and Nait-Saada A 1981 *Solid State Commun.* **37** 741
[18] Barthem V M T S, Gignoux D, Schmitt D and Creuzet G 1989 *J. Magn. Magn. Mater.* **78** 56
[19] Radwański R J and Franse J J M 1992 *Physica* B **177** 193